Analyst

Accepted Manuscript

ROYAL SOCIETY OF CHEMISTRY

www.rsc.org/analyst

The biochemical changes in the hippocampal formation occurring in normal and seizure experiencing rats as a result of ketogenic diet

Joanna Chwiej[1*], Agnieszka Skoczen[1], Krzysztof Janeczko[2], Justyna Kutorasinska[1], Katarzyna Matusiak[1], Henryk Figiel[1], Paul Dumas[3], Christophe Sandt[3] and Zuzanna Setkowicz[2]

[1] AGH-University of Science and Technology, Faculty of Physics and Applied Computer Science, Krakow, Poland

[2] Jagiellonian University, Institute of Zoology, Krakow, Poland

[3] SOLEIL, St Aubin, France

Corresponding author:

Joanna Chwiej

AGH University of Science and Technology

al. Mickiewicza 30, 30-059 Krakow, Poland

Phone: +48 12 617 41 55, Fax: +48 12 634 00 10

joanna.chwiej@fis.agh.edu.pl

Keywords: temporal lobe epilepsy, pilocarpine model, ketogenic diet, SRFTIR microspectroscopy and imaging, biochemical analysis

Abstract

In this study, ketogenic diet-induced biochemical changes occurring in normal and epileptic hippocampal formations were compared. Four groups of rats were analyzed, namely seizure experiencing animals and normal rats previously fed with ketogenic (KSE and K groups respectively) or standard laboratory diet (NSE and N groups respectively). Synchrotron radiation based Fourier-transform infrared microspectroscopy was used for the analysis of distributions of main organic components (proteins, lipids, compounds containing phosphate group(s)) and their structural modifications as well as anomalies in creatine accumulation with micrometer spatial resolution.

Infrared spectra recorded in molecular layers of dentate gyrus (DG) areas of normal rats on ketogenic diet (K) presented increased intensity of 1740 cm^{-1} absorption band. This is originating from the stretching vibrations of carbonyl groups and probably reflects increased accumulation of ketone bodies occurring in animals on high fat diet compared to those fed with standard laboratory diet (N). The comparison of K and N groups showed, moreover, elevated ratios of absorbance at 1634 and 1658 cm^{-1} for DG internal layers and increased accumulation of creatine deposits in sector 3 of Ammon's horn (CA3) hippocampal area of ketogenic diet fed rats.

In multiform and internal layers of CA3, seizure experiencing animals on ketogenic diet (KSE) presented lower ratio of absorbance at 1634 and 1658 cm^{-1} comparing to rats on standard laboratory diet (NSE). Moreover, in some of the examined cellular layers increased intensity of the 2924 cm^{-1} lipid band as well as the massifs of 2800-3000 cm^{-1} and 1360-1480 cm^{-1} was found in KSE comparing to NSE animals. The intensity of 1740 cm^{-1} band was diminished in DG molecular layers of KSE rats. Ketogenic diet did not modify the seizure induced anomalies in unsaturation level of lipids as well as number of creatine deposits.

Introduction

Epilepsy is one of the most common serious neurological disorder.[1] It is characterized by spontaneous recurrent seizures, caused by focal or generalized paroxysmal changes in neurological functions triggered by abnormal electrical activity of nerve cells.[2]

In around 40% of epilepsy cases, disease etiology is known and the most frequent causes of acquired epilepsies are brain insults including traumatic brain injury, ischemic stroke, intracerebral hemorrhage, infections, tumors, cortical dysplasia, neurodegenerative diseases, and prolonged acute symptomatic seizures.[3] Although people at risk of epilepsy can be identified, there is still no prophylactic treatment that would prevent the development of the disease.[4,5]

Despite continued advancements in anticonvulsant development, approximately 20-40% of patients with epilepsy have refractory seizures,[6] and so remains a significant demand for additional solutions. A growing body of evidence demonstrates that dietary therapies for this disease (classic ketogenic diet, medium-chain triglyceride diet, modified Atkins diet and low-glycemic-index treatment) are highly effective, with approximately 30-60% of children overall having at least a 50% reduction in seizures after 6 months of treatment.[7,8,9,10] All these dietary therapies share the common characteristic of restricting carbohydrate intake to shift the predominant caloric source of the diet to fat.[11] Catabolism of fats results in the production of ketone bodies which are alternate energy substrates to glucose.[12] Although many mechanisms by which ketone bodies yield its anticonvulsant effect are proposed, the relationships between the brain metabolism of the ketone bodies and their neuroprotective and antiepileptogenic action in case of epilepsy still remain to be disentangled.[12]

In this paper, the mechanisms of ketogenic diet action in epileptic hippocampal formation were examined. The rat pilocarpine model of temporal lobe epilepsy (TLE) was used in the study. Such choice resulted from the two factors. Mainly, this animal model of TLE belongs to the group of models recommended by the National Institute of Health/National Institute of Neurological Disorders and Stroke, as the most useful for examination of new antiepileptogenic and disease-modifying therapies. Moreover, this model of seizures was widely examined in our previous papers.[13,14,15,16,17,18,19,20]

Our earlier research showed, inter alia, that excitotoxicity, mossy fibers sprouting, iron catalyzed oxidative stress and decreased enzymatic activity of creatine kinase should be taken into account as important phenomena involved in neurodegenerative changes of hippocampal formation and spontaneous seizure activity in the chronic phase of pilocarpine model of seizures.[13,14,17,18,19] The knowledge of the pathogenesis of epilepsy and the appropriate analytical tools allow us entering the next phase of the research, namely looking for neuroprotective and antiepileptogenic therapies.

The highly resolved biochemical analysis of hippocampal formations taken from ketogenic diet fed rats experiencing seizures may shed some new light on the processes of its possible neuroprotective action in epileptic brain. Such biochemical data including the distributions of main organic compounds (proteins, lipids, nucleic acids) as well as their conformational changes may be obtained using synchrotron Fourier transform infrared (SRFTIR) microspectroscopy. The technique is a combination of light microscopy and infrared spectroscopy. With the first method we are able to localize microscopic details in the analyzed samples, while the second one provides information concerning its chemical composition. The high brightness of synchrotron source of infrared radiation causes that high spatial resolution images at or near the diffraction limit can be obtained with better S/N and shorter data collection time than if a thermal source is used.[21] It makes such IR source especially valuable, when highly spatially resolved analysis of samples is necessary.[21,22] Because in biomedical research micrometer spatial resolution is often of great importance, synchrotron-based FTIR microspectroscopy is becoming a more and more desired analytical tool in case of investigation of different biological systems.[23,24,25,26]

In this paper the influence of ketogenic diet on the biochemical composition of hippocampal formations in normal and seizure experiencing rats will be analyzed. The subject of the study will be the changes in the accumulation and structure of proteins, lipids and compounds containing phosphate group(s)) as well as anomalies in creatine accumulation.

High spatial resolution plays an important role also in our studies. Based on our experience, we know that seizure induced anomalies in the distribution of biomolecules can be limited to specific cellular layers of hippocampal formation and the typical size of hippocampal creatine inclusions varies from a few to dozens of micrometers. Because of these facts, it is necessary to use characterization technique which combines high spatial resolution (micrometer scale) with high biochemical (spectral) sensitivity. Without a doubt, FTIR micro-spectroscopy with synchrotron source of infrared radiation fulfills these requirements.

Materials and methods

Animals

Male Wistar rats originated from an animal colony of the Department of Neuroanatomy (Institute of Zoology, Jagiellonian University). All animal-use procedures were carried out there and were approved by the Bioethical Commission of the Jagiellonian University in accordance with international standards.

Four groups of rats were examined in the study and their characteristics are reported in the Table 1.

Table 1. The characteristic of examined animal groups

Experimental group	Ketogenic diet*	Standard diet	Pilocarpine**	Perfusion***
N (n=4)****		+		+
K (n=5)	+			+
NSE (n=5)		+	+	+
KSE (n=5)	+		+	+

*ketogenic diet was introduced to rats on the 30th day of their postnatal life;
**Pilocarpine was injected to rats on the 60th day of postnatal development;
***Perfusion with physiological saline solution was done on the 60th day of rat postnatal life;
**** n – the number of animals in experimental group.

From the day 30th of postnatal development the animals were fed either with ketogenic (K and KSE groups) or standard laboratory diet (N and NSE groups). The content of main nutrients in ketogenic and standard diet are compared in the Table 2.

Table 2. The content of main nutrients (in [%]) in the dry mass of ketogenic and standard diet

Nutrient	Ketogenic diet	Standard diet
Lipids	75*	5
Carbohydrates	5	63
Proteins	9	25
Others	11	7

* lard (61%) and soybean oil (14%).

Seizure induction

In order to induce seizures, the rats from groups NSE and KSE received a single i.p. injection of pilocarpine (250 mg/kg, Sigma P6503) on 60th day of their postnatal development. Additionally, they were injected with scopolamine methyl bromide (1 mg/kg, Sigma S8502) 30 min prior to pilocarpine to reduce its peripheral effects. The mentioned procedures were done between 9 and 10 a.m. to avoid circadian changes in seizure vulnerability.

Behavioral observations

During the 6-h long period after pilocarpine injection, the animals were continuously monitored by an observer unaware of their previous experimental treatment. The motor seizures intensity was rated on a 6-point scale with respect to the symptoms and their intensity. The scale was applied in our previous study[27] and corresponded to that introduced by Racine[28] and widely used in studies on animal models of epilepsy. During the observation period, general parameters of the status epilepticus also were recorded. They included: the latency of the first motor seizure sign, the maximal intensity of seizures and the total time of seizure activity within the observation period.

Sample preparation

Six hours after epilepsy induction, all animals were perfused with physiological saline solution of high analytical purity. Afterwards, the brains were immediately excised from the skulls and snap-frozen in liquid nitrogen. No OCT (optimal cutting temperature) compounds

were used before cutting with a cryomicrotome. The obtained in the cryomicrotome 12 μm thick slices with the dorsal part of the hippocampal formation[29] were placed on MirrIR low-e microscopic slides and stored at -70°C till the measurements. In order to avoid freeze-thaw damages of tissues the temperature was increased steadily from -70°C to the room temperature in which we analyzed the samples. Such sample preparation allowed us to avoid the use of fixative media and paraffin having IR spectral signatures that can mask absorption bands of biological components.[30].

According to the recently published papers, transflection measurements done on reflective substrates may be connected with the electric field standing wave artefacts.[31,32,33] Nevertheless, the measurements were done in transflection mode and MirrIR slides were used as sample carriers. The main reason of such choice was the possibility of comparison and verification of the obtained results in respect of our previous studies done on pilocarpine model of seizures. In the work of Wehbe *et al.*[32] it was showed how crucial it is for the comparative biochemical studies that all samples are measured on the same substrate type.

IR data collection

SRFTIR microspectroscopy was used for biochemical analysis of rat brain samples. The experiment was done at SMIS beamline of SOLEIL synchrotron facility. The measurements were cariied out in transflection mode using an infrared microscope Continuum XL equipped with a 32xmagnification/0.6 numerical aperture Schwarzschild objective. The microscope was coupled to a FTIR spectrometer ThermoNicolet 5700 equipped with a 50 μm MCT detector. The 12-μm thick cryomicrotome samples deposited on MirrIR slides were analyzed using the IR beam of 10x10 μm^2 – defined by a knife-edge aperture. The step size used during raster scanning of samples was equal 10 micrometers in both directions. The spectral resolution was set to 6 cm^{-1} and 38 scans were averaged per sample spectrum. Each background spectrum was collected co-adding 128 scans. The data acquisition as well as spectral analysis was done with OMNIC software (Version 8.0).

Analysis of spectral data

The univariate spectral maps were performed by displaying either the area of one peak or the area ratio for the two peaks. Trapezoidal baseline corection was done during calculations of integrated peak areas. Typically, background was taken at the two extreme frequency values of the peaks. There were two exeptions to this rule. They concerned the spectral bands occurring within the lipid (wavenumber region 2800-3000 cm^{-1}) and amide (wavenumber region 1480-1770 cm^{-1}) massifs. For these bands the linear baseline was taken at frequencies corresponding to the beginning and the end of massifs.

Chemical mapping was carried out on unprocessed spectra. Before detailed quantitative and statistical analysis we verified the quality of the spectra focusing on the two main problems i.e. sample thickness and the presence of Mie scattering induced artifacts. The thickness tests were done in the CytoSpec software using the criteria proposed by Lasch *et al.*[34]

The layered character of the analyzed tissues may result in the differences of optical densities between the specific cellular layers and these differences, in turn, may cause in the IR absorption spectra artifacts connected with the presence of resonant and non-resonant Mie scattering (RMieS and EMSC respectively) phenomena. According to Bassan *et al.*[35] the three main dispersion artifacts, being the result of Mie scattering, which should be taken into account, are:

1. a broad hump in the baseline between 2000 and 4000 cm^{-1},
2. a sharp decrease in the absorbance for 1750 cm^{-1} (RMieS),
3. a downward shift in the true position of amide I band.

The occurrence of the mentioned artifacts, and particularly the last one, may influence the shape of the amide I band and the same the parameters being the measures of changes in secondary structure of proteins. Therefore, the IR spectra recorded for samples were tested for the presence of the three above mentioned artifacts. Some influence of Mie scattering phenomena on the recorded spectra was noticed only for the tissue areas situated on the borders of different cell layers. The results of chemical mapping done for the spectra affected through Mie scattering were not taken into account in further analyses.

Statistical analysis

The Mann-Whitney U test was applied for statistical evaluation of the differences between animal groups under analysis. The choice of non-parametric statistical test resulted from the fact that our data could not meet the assumptions about normality, homoscedasticity and linearity which are necessary for the use of its parametric alternative. As it was mentioned before, typically, experimental groups consisted of five rats. One slice of the dorsal part of the hippocampal formation per each animal was examined using FTIR microspectroscopy.

Results

Two areas of the hippocampal formation, the sector 3 of Ammon's horn (CA3) and the dentate gyrus (DG), were chosen for investigation. Infrared absorption spectra for each pixel were recorded by simple moving the sample in the plane perpendicular to the IR beam. The typical spectrum obtained for hippocampal tissue sample is presented in the Figure 1. Additionally, in the Table 3, the tentative assignments of the bands frequencies characteristic for IR spectra measured for nervous tissue samples are listed.

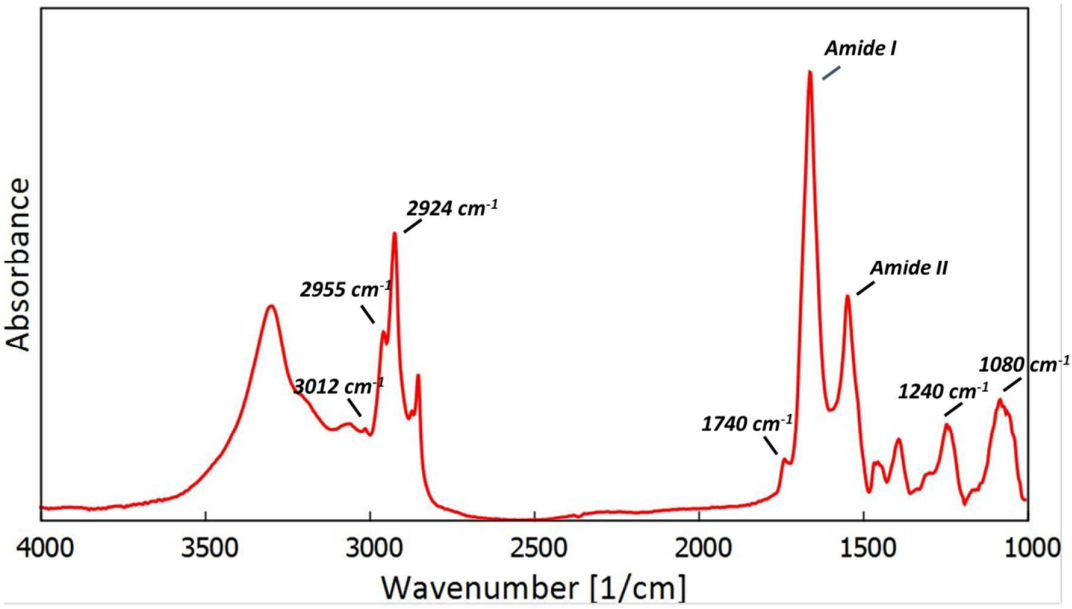

Figure 1. The typical spectrum (baseline corrected) recorded for the hippocampal formation tissue.

Table 3. The tentative assignments of the bands frequencies characteristic for IR spectra measured for nervous tissue samples[36,37]

Frequency [cm^{-1}]	Assignment
~3300	amide A: N-H str in resonance with (amide II harmonic) (proteins)
~3110	amide B: N-H str in resonance with (amide II harmonic) (proteins)
~3010	=C-H str (unsaturated fatty acids)
~2956	CH_3 asym str (lipids and proteins)
~2920	CH_2 asym str (lipids)
~2870	CH_3 sym str (lipids and proteins)
~2850	CH_2 sym str (lipids)
~1730	C=O str (phospholipids, cholesterol ester)
~1640-1653	amide I band: C=O str, C-N str, N-H bend (proteins, sphingolipids)
~1545-1567	amide II: N-H bend, C-N str (proteins, sphingolipids)
1485	$(CH_3)_3N^+$ asym bend (lipids)
~1460-1473	CH_2 sciss, CH_3 asym bend (lipids)
~1443	CH_2 (cyclic) sciss (cholesterol, cholesterol ester, DAG, TAG)
~1378	CH_3 sym bend (lipids)
~1365	CH_2 sym bend (lipids)
~1200-1400	amide III: C-N str, N-H bend, C=O str, O=C-N bend (proteins)
~1228-1244	PO_2 asym str (nucleic acids, phospholipids)
~1170	CO-O-C asym str (phospholipids)
~1084-1089	PO_2 sym str (nucleic acids, phospholipids)

str – stretching; asym – asymmetric; sym – symmetric; bend – bending; sciss – scissoring

For all the analyzed samples the two-dimensional maps of selected functional groups were computed. The detailed list of examined absorption bands (and their ratios) is reported in the Table 4.

Table 4. Absorption bands (the ratios of absorption bands) analyzed in the study

Absorption band (ratio of absorption bands)	Remarks
1658 cm^{-1}	amide I band, distribution of proteins
1545 cm^{-1}	amide II band, distribution of proteins
1545 cm^{-1}/1658 cm^{-1}	structural changes of proteins [a]
1634 cm^{-1}/1658 cm^{-1}	
1080 cm^{-1}	distribution of compounds containing phosphate groups(s) including nucleic acids, phospholipids, phosphorylated carbohydrates, differences in the degree of phosphorylation of carbohydrates and/or glycoproteins [b]
1240 cm^{-1}	
1360-1480 cm^{-1}	distribution of lipids, cholesterol esters, cholesterol
1740 cm^{-1}	distribution of phospholipids, cholesterol esters, ketone bodies [c]
2924 cm^{-1}	distribution of lipids
2955 cm^{-1}	distribution of lipids
2800-3000 cm^{-1}	lipid massif, distribution of lipids
3012 cm^{-1}	distribution of unsaturated fatty acids
3012 cm^{-1}/2924 cm^{-1}	unsaturation level of lipids [d]
3012 cm^{-1}/2800-3000 cm^{-1}	
3012 cm^{-1}/1658 cm^{-1}	unsaturated lipids/proteins ratio
2924 cm^{-1}/2955 cm^{-1}	saturation level of lipids [d], changes in length of fatty acids chains and the degree of their branching [e]
1080 cm^{-1}/2924 cm^{-1}	compounds containing phosphate bond(s)/lipids ratio
1240 cm^{-1}/2924 cm^{-1}	
1080 cm^{-1}/2800-3000 cm^{-1}	
1240 cm^{-1}/2800-3000 cm^{-1}	
1080 cm^{-1}/1658 cm^{-1}	compounds containing phosphate bond(s)/proteins ratio
1240 cm^{-1}/1658 cm^{-1}	
1360-1480 cm^{-1}/1658 cm^{-1}	ratios of appropriate biological compounds
1360-1480/2800-3000 cm^{-1}	
1740 cm^{-1}/2924 cm^{-1}	
1740 cm^{-1}/2800-3000 cm^{-1}	
1740 cm^{-1}/1658 cm^{-1}	
2924 cm^{-1}/1658 cm^{-1}	lipids/proteins ratio
2800-3000 cm^{-1}/1658 cm^{-1}	
1304 cm^{-1}	creatine distribution [f]
1398 cm^{-1}	
2800 cm^{-1}	

[a] from Kneipp *et al.*, 2003;[38] Miller et al., 2006;[39] Kretlow *et al.*, 2006;[40] Szczerbowska-Boruchowska *et al.*, 2007;[41] Chwiej *et al.*, 2010;[14]

[b] from Kneipp *et al.*, 2000;[42] Diem *et al.*, 1999;[43] Liquier & Taillandier, 1996;[44] Szczerbowska-Boruchowska *et al.*, 2007;[41]

[c] from NIST Standard Reference Database Number 69;[45]

[d] from Petibois & Deleris, 2005;[46] Petibois & Deleris, 2006;[47]

[e] from Kretlow A, 2007;[48] from Dogan *et al.*, 2013;[49]

[f] from Gallant *et al.*, 2006;[50] Dulinska *et al.*, 2012;[18] Kutorasinska *et al.*, 2013.[20]

During the ketogenic diet delivery, energy is mainly derived from fats which are converted to the following ketone bodies: β-hydroxybutyrate, acetoacetate and acetone. All of them quite easily cross the blood–brain barrier either by simple diffusion (acetone) or with the aid of monocarboxylic transporters (β-hydroxybutyrate, acetoacetate).[51] Therefore, in the Table 5 the main absorption bands of the mentioned ketone bodies were compared with those specific to glucose and cholesterol which can also change during high fat diet.

Table 5. Absorption bands of ketone bodies, cholesterol and glucose occurring within the examined wavenumber region[45]

Compound					Influenced analytical band
β-hydroxybutyrate	Acetoacetate	Acetone	cholesterol	D-glucose	
2900-3000 cm^{-1}	-	2923 cm^{-1} 2966 cm^{-1} 3000 cm^{-1}	2800-3000 cm^{-1}	2900 cm^{-1}	2800-3000 cm^{-1}
1770 cm^{-1}	1750 cm^{-1}	1720 cm^{-1}		-	1740 cm^{-1}
1360 cm^{-1}	-	1360 cm^{-1}	1380 cm^{-1} 1450 cm^{-1}	1360 cm^{-1} 1420 cm^{-1}	1360-1480 cm^{-1}
1200 cm^{-1}	1240 cm^{-1}	1220 cm^{-1}	-	1220 cm^{-1}	1240 cm^{-1}
-	-	-	1050 cm^{-1}	1000 cm^{-1} 1050 cm^{-1}	1080 cm^{-1}

In the Figures 2 and 3 the exemplary results of chemical mapping done for selected DG and CA3 hippocampal areas are shown. The univariate maps were obtained as described previously in the part *Analysis of spectral data*.

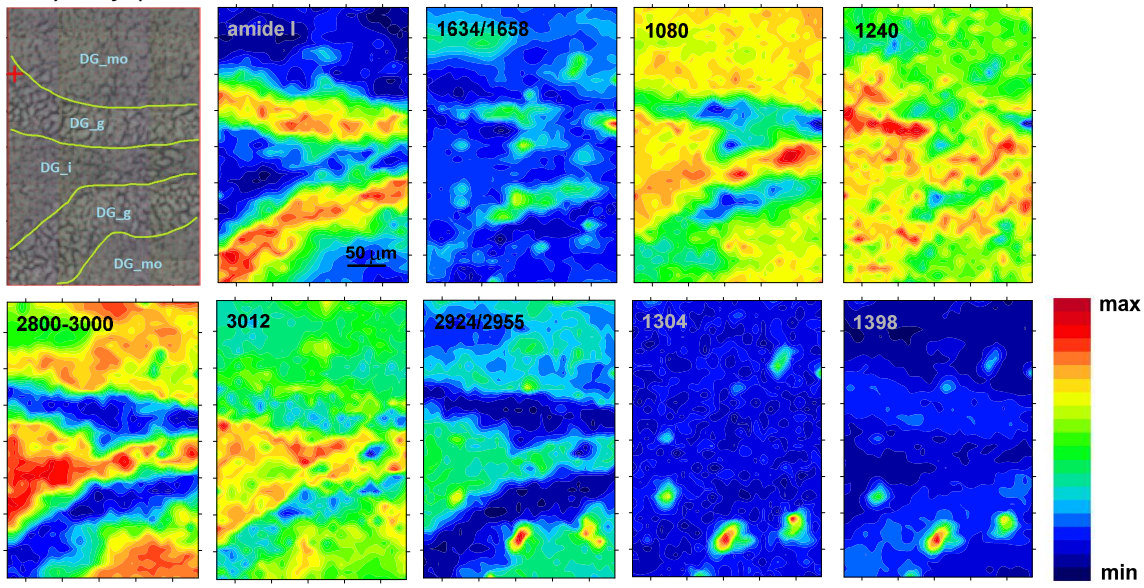

Figure 2. The comparison of chemical maps obtained for DG area taken from selected KSE animal with the microscopic view of the scanned tissue. DG_mo, DG_g, DG_i – molecular, granular and internal cellular layers of DG area. The data were interpolated using Kriging method.

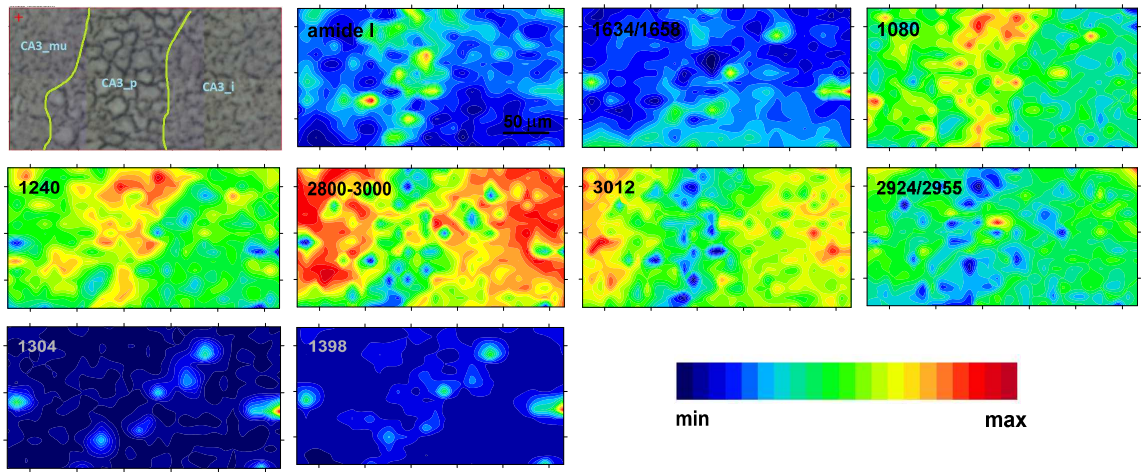

Figure 3. The comparison of chemical maps obtained for CA3 area taken from selected KSE animal and superimposed with the visual image of the scanned tissue. CA3_mu, CA3_p and CA3_i – multiform, pyramidal and internal cellular layers of CA3 area. The data were interpolated using Kriging method.

For all analyzed samples the chemical maps were superimposed on the microscopic views of the corresponding tissue areas (as shown in the Figures 2 and 3) to identify cellular layers taken for further detailed analysis. These were pyramidal (CA3_p), internal (CA3_i) and multiform (CA3_mu) layers in case of CA3 and granular (DG_g), internal (DG_i) and molecular (DG_mo) layers in case of DG hippocampal area. For each examined animal, 25 representative spectra were chosen from the six mentioned above cellular layers. The spectra were used to calculate the mean intensities of selected absorption bands and their average ratios. The intensities of bands were evaluated on the same way as it was done in the chemical mapping process what was widely described in the part *Analysis of spectral data*.

In order to compare the animals from examined experimental groups and evaluate the statistical significance of the differences in biochemical composition between them, the medians for K, N, KSE and NSE groups of rats were used.

Influence of ketogenic diet on the normal hippocampal formation

To analyze the effect of ketogenic diet on accumulation of biomolecules in the normal hippocampal formation, the median values of biochemical parameters obtained for K and N groups were compared (see Table 1S of supplementary materials). The statistical significance of differences between the animal groups was evaluated using non-parametric U Mann-Whitney test and its results are presented in the Table 1S. The dispersions of parameters which significantly differed between animals fed with ketogenic or standard laboratory diet are shown as box-and-whisker plots in the Figure 4.

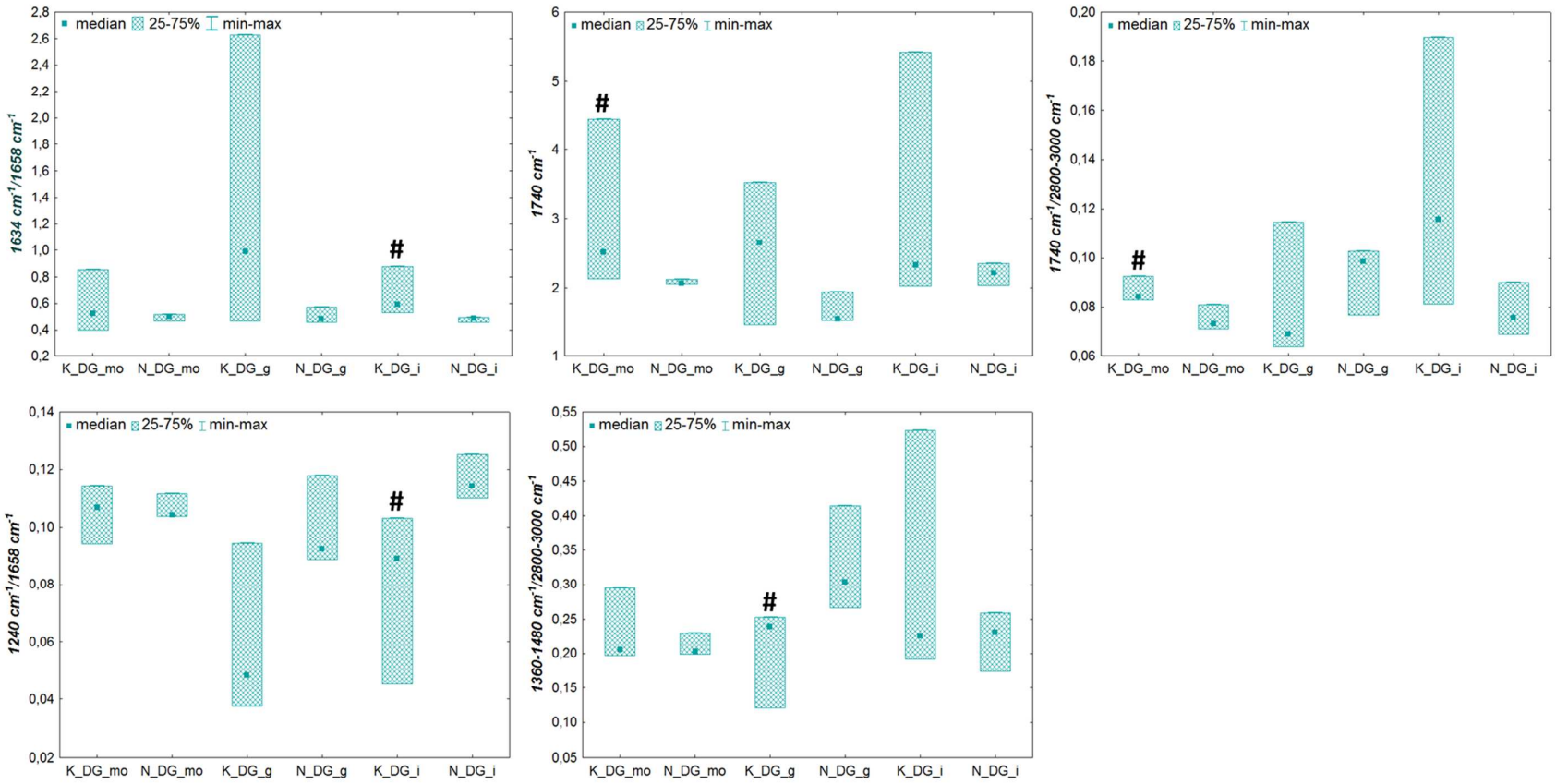

Figure 4. Median, minimal and maximal values (after the removal of outliers) of biochemical parameters presenting differences between normal animals on ketogenic (K) and standard (N) laboratory diet. The cellular layers for which statistically significant changes after the treatment with ketogenic diet occurred (U Mann-Whitney test at the significance level of 10%) were marked with (#).

As one can notice from the Table 1S and Figure 4, a few differences (significant at the level of 10%) were found between cellular layers of DG areas representing K and N groups.
No statistically significant changes were observed between CA3 areas of normal rats fed with ketogenic and standard diet. Statistically significant increase in the ratio of absorbance at 1634 and 1658 cm^{-1} was found for ketogenic diet fed animals in the internal layer of DG. It can be verified in the Figure 5 (part I) where the absorption spectra recorded in the mentioned cellular layer for selected rat on ketogenic (spectrum B) and standard laboratory diet (spectrum A) were compared.

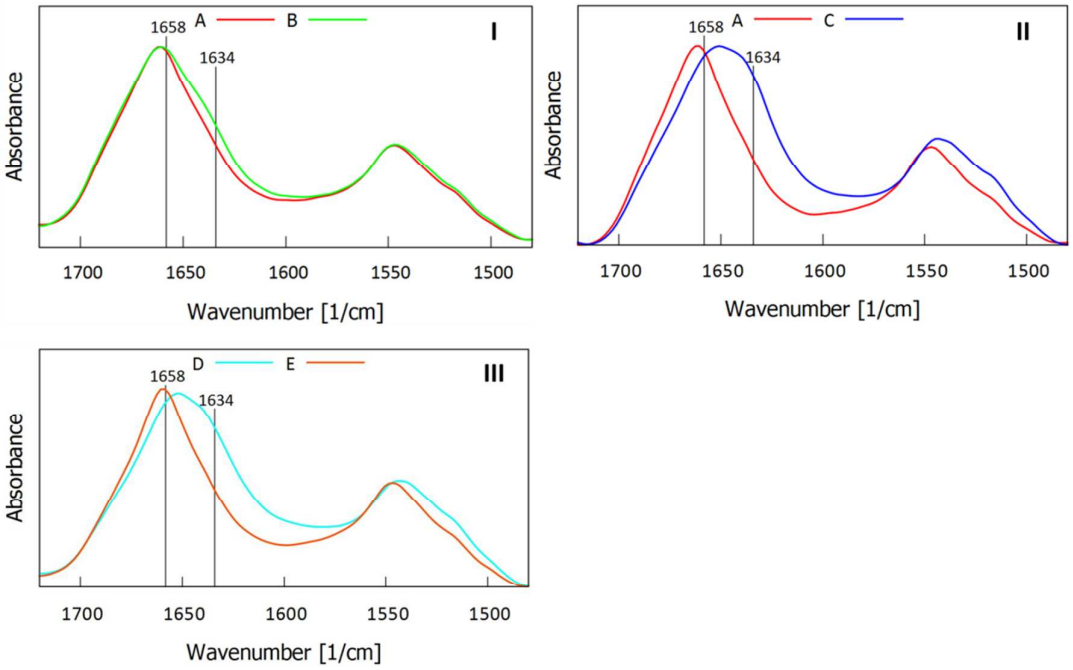

Figure 5. The comparison of absorption spectra (amide I-amide II region) recorded in internal layer of DG area from selected animals representing N (spectrum A), K (spectrum B) and NSE (spectrum C) groups (parts I and II). The comparison of spectra measured in multiform layer of CA3 for selected rats from NSE (D) and KSE (E) groups.

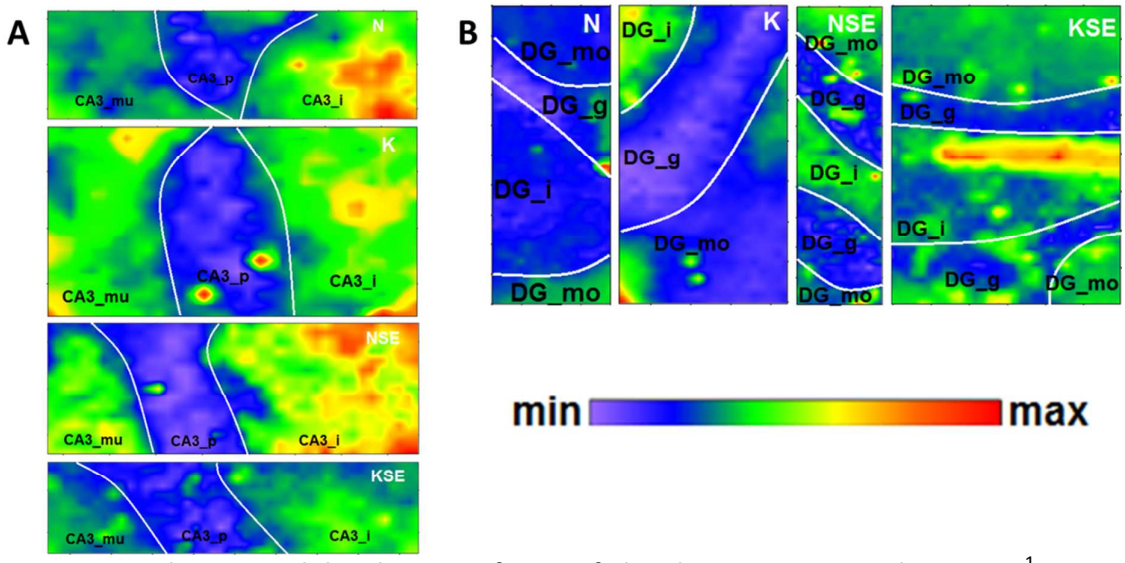

Figure 6. Two dimensional distributions of ratio of absorbance at 1634 and 1658 cm^{-1} in CA3 (A) and DG (B) areas from selected samples representing N, K, NSE and KSE groups.

The comparison of K and N animals showed, moreover, an increased intensity of the band occurring at 1740 cm^{-1} in molecular layer of DG. To demontrate this result, in the Figure 7 the two-dimesional distributions of 1740 cm^{-1} absorption band in DG areas from selected K and N rats were presented. Moreover, the example absorption spectra (focused on the 1740 cm^{-1} absorption band) recorded in molecular layers of these areas were compared there.

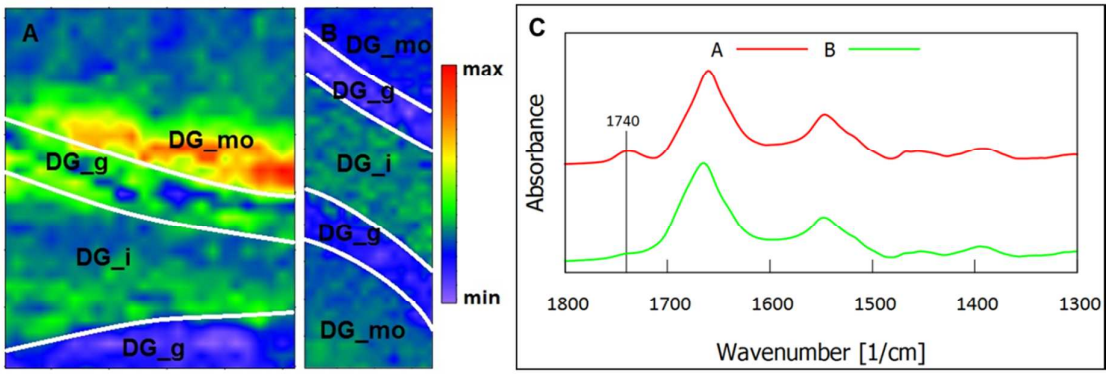

Figure 7. The distributions of 1740 cm^{-1} absorption band in DG areas from selected K (A) and N (B) animals. C – the comparison of absorption spectra (after linear baseline correction) recorded in molecular layers of A nad B DG areas (in red – spectrum recorded for ketogenic diet fed normal rat, in green – spectrum measured for standard diet fed normal rat).

Influence of seizures on the normal hippocampal formation

To verify the influence of ketogenic diet on the epileptic hippocampal formation first we needed to know how seizures modify this brain area in rats fed with the standard laboratory diet. Seizure-induced biochemical changes in the hippocampal formation were the subject of our previous studies which revealed a few significant anomalies in animals treated with pilocarpine.[14,18,20] They involved structural changes of proteins and lipids as well as increased accumulation of creatine deposits within epileptic hippocampal formation.

The effect of seizures on the biochemical state of hippocampal formation was analyzed through the comparison of biomolecular parameters recorded for pilocarpine treated (NSE)

and normal (N) animal groups both fed with the standard laboratory diet. The medians of band intensities (or their ratios) evaluated for these two groups of rats are listed in the Table 2S of supplementary materials. Additionally, in Figures 8a and 8b the dispersions of biochemical parameters which significantly differed between NSE and N animals are shown as box-and-whisker plots.

As it can be seen from the Table 2S and Figures 8a-b, seizures induced many changes of biochemical parameters in animals on standard laboratory diet. Similarly as in our previous studies, an increased ratio of absorbance at 1634 and 1658 cm^{-1} was found for animals with pilocarpine evoked seizures. These anomalies were statistically significant in molecular and internal layers of DG. Seizure induced changes in the amide I band can be easily noticed in the Figure 5 (part II) where the spectra recorded for internal layer of DG for selected NSE (spectrum C) and N (spectrum A) animals were compared.

For NSE rats the ratio of intensity of bands 2924 and 2955 cm^{-1} was elevated for the internal layer of CA3. Moreover, animals treated with pilocarpine presented lower unsaturation level of lipids which was monitored through the ratios of intensities of bands 3012 cm^{-1}/2924 cm^{-1} and 3012 cm^{-1}/2800-3000 cm^{-1}. However, the changes in lipids unsaturation were also statistically significant only in the internal layer of CA3 area. For some of the analyzed cellular layers we also observed a decrease of the intensity of absorption for bands occurring at 1740, 1240 and 1080 cm^{-1} in NSE comparing to normal rats.

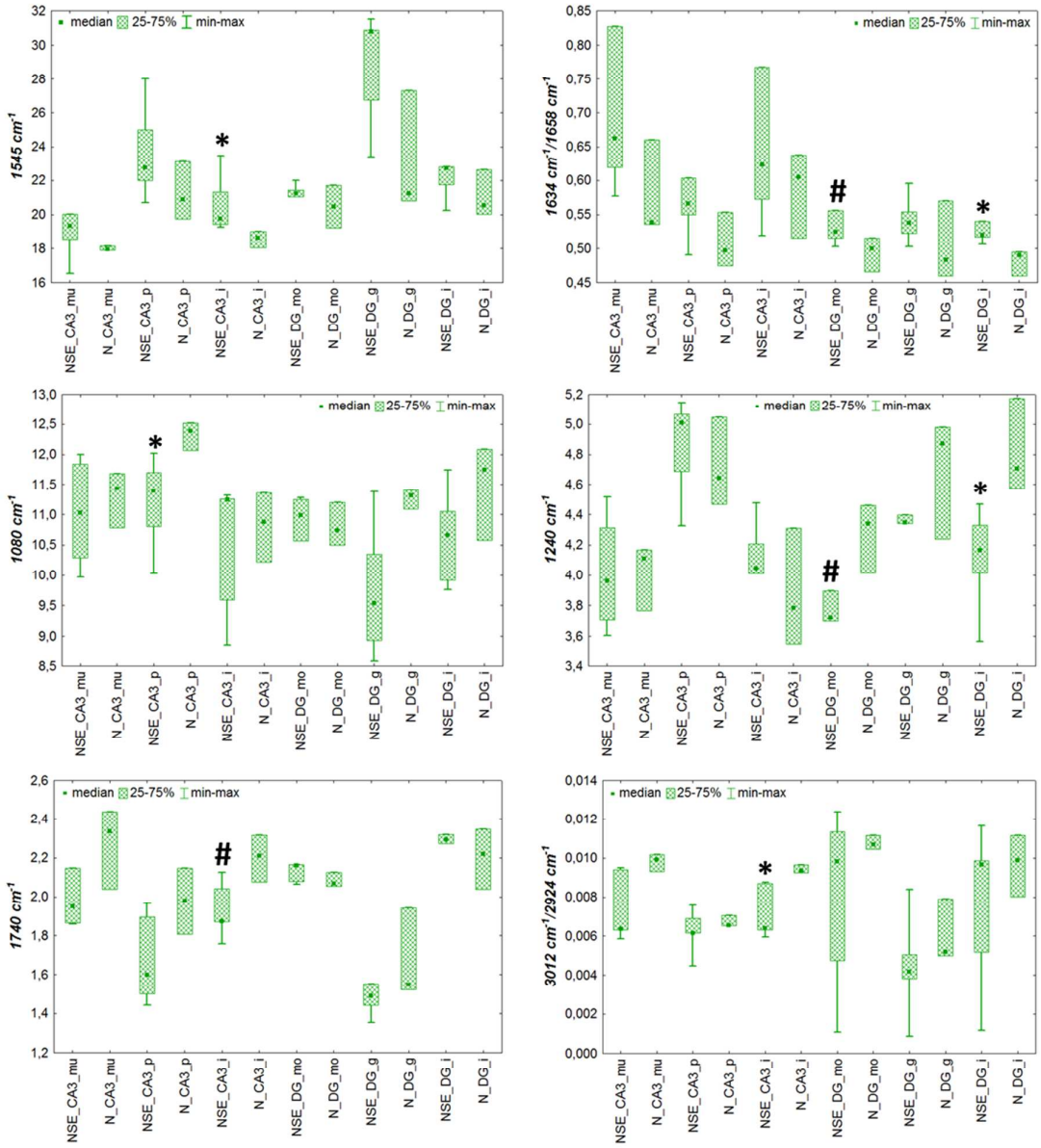

Figure 8a. Median, minimal and maximal values (after the removal of outliers) of biochemical parameters presenting differences between NSE and N groups. The cellular layers for which statistically significant changes were observed at the confidence level of 95% were marked with (*) whilst those significant at the confidence level of 90-95% with (#).

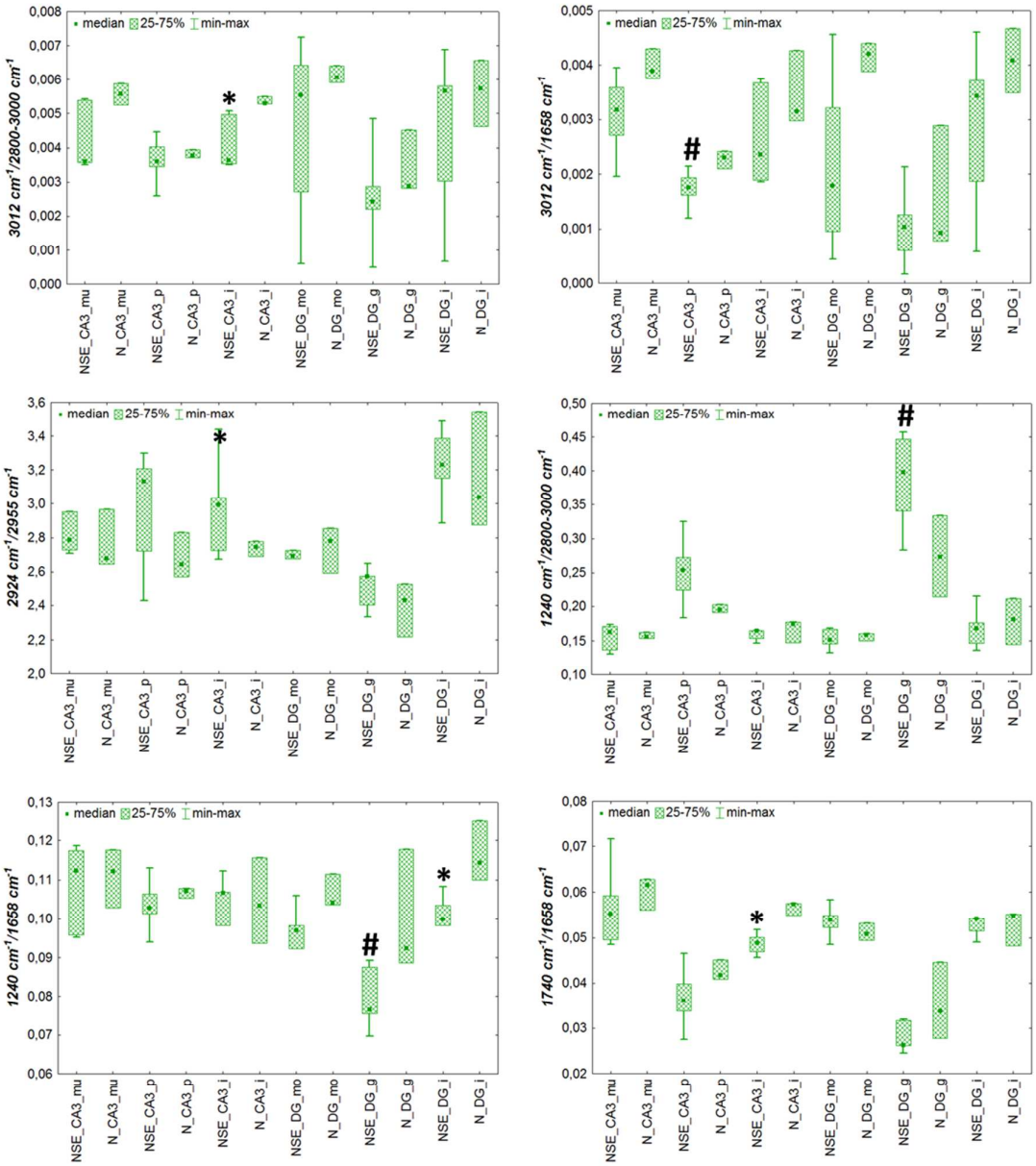

Figure 8b. Median, minimal and maximal values (after the removal of outliers) of biochemical parameters presenting differences between NSE and N groups. The cellular layers for which statistically significant changes were observed at the confidence level of 95% were marked with (*) whilst those significant at the confidence level of 90-95% with (#).

Influence of ketogenic diet on seizure experiencing brain

Analysis of ketogenic diet impact on the epileptic brain was based on the comparison of biochemical parameters achieved for seizure experiencing rats on ketogenic (KSE) or standard (NSE) laboratory diets. The data obtained for both animal groups are presented in the Table 3S of supplementary materials and in Figures 9a and 9b where the dispersions of biochemical parameters which significantly differed between KSE and NSE animals are shown as box-and-whisker plots.

The obtained results clearly show that ketogenic diet modifies biochemical anomalies occurring in the hippocampal formation as a result of pilocarpine evoked seizures. In seizure

experiencing animals on ketogenic diet a lower ratio of absorbance at 1634 and 1658 cm^{-1} was observed comparing to that in rats on standard laboratory diet. Such result was statistically significant only in case of multiform and internal layers of CA3. As an example, in the Figure 5 (part III), the absorption spectra measured in CA3 multiform layer for selected rats representing NSE (spectrum D) and KSE (spectrum E) groups were demonstrated.

For some of the examined cellular layers an increased intensity of 2924 cm^{-1} band (in internal layer of CA3, molecular and granular layers of DG) and massifs occurring at the wavenumber ranges of 2800-3000 cm^{-1} (in pyramidal layer of CA3, molecular and granular layers of DG) and 1360-1480 cm^{-1} (in multiform layer of CA3 and molecular of DG)was found in KSE comparing to NSE animals. The intensity of 1740 cm^{-1} band was diminished in multiform layer of DG area. The ratios of intensities 1080/2924 cm^{-1} and 1080/2800-3000 cm^{-1} decreased in pyramidal layer of CA3 and molecular and granular layers of DG areawhat probably resulted from the increased lipid content in animals on ketogenic diet. Similar but more considerable relations were found for the ratios of 1740/2924 cm^{-1} and 1740/2800-3000 cm^{-1} (in cellular layers of DG area) and may be also an effect of increased lipid accumulation or diminished content of ketone bodies utilized as an energy source during seizures.

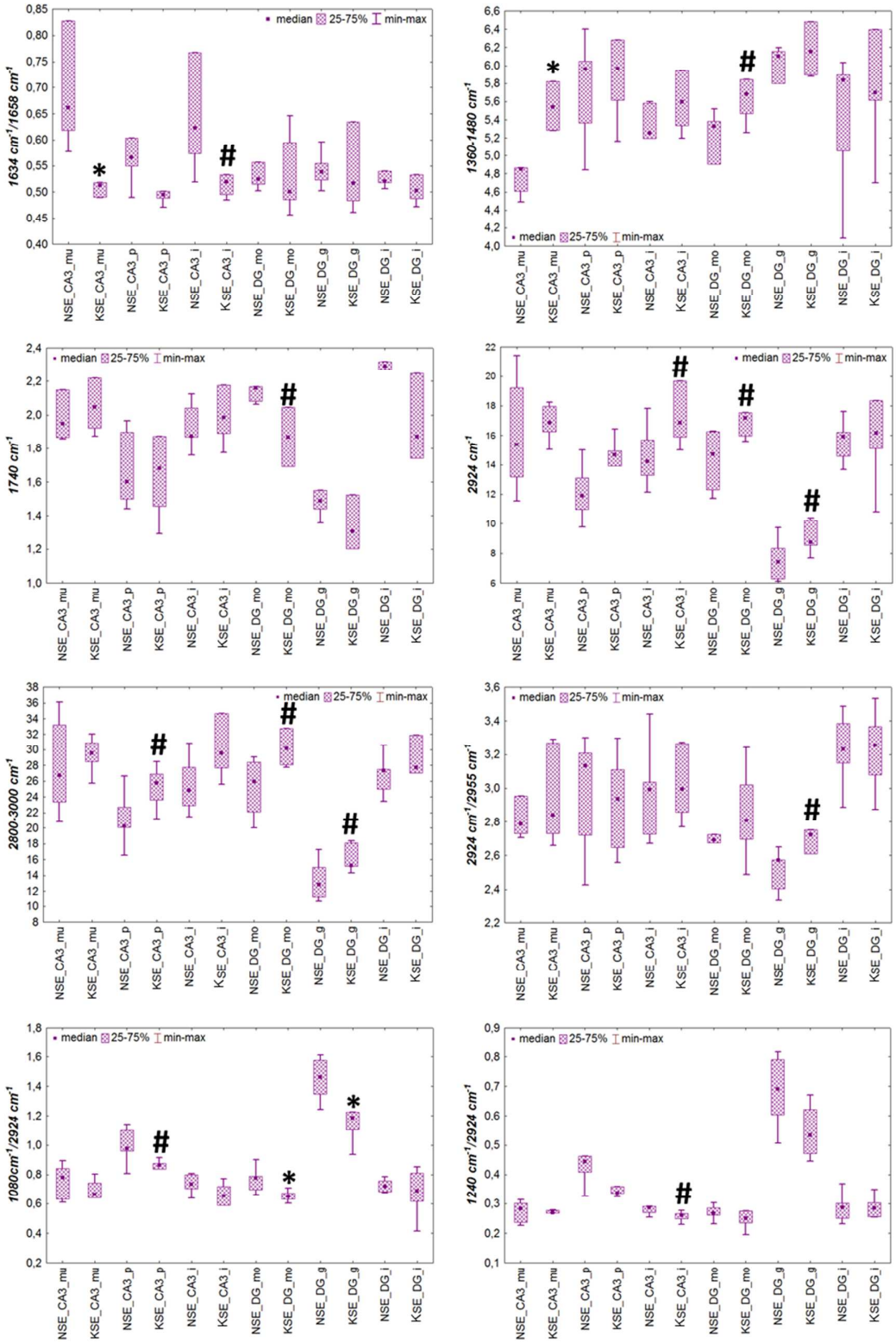

Figure 9a. Median, minimal and maximal values (after the removal of outliers) of biochemical parameters presenting differences between KSE and NSE groups. The cellular layers for which statistically significant changes were observed at the confidence level of 95% were marked with (*) whilst those significant at the confidence level of 90-95% with (#).

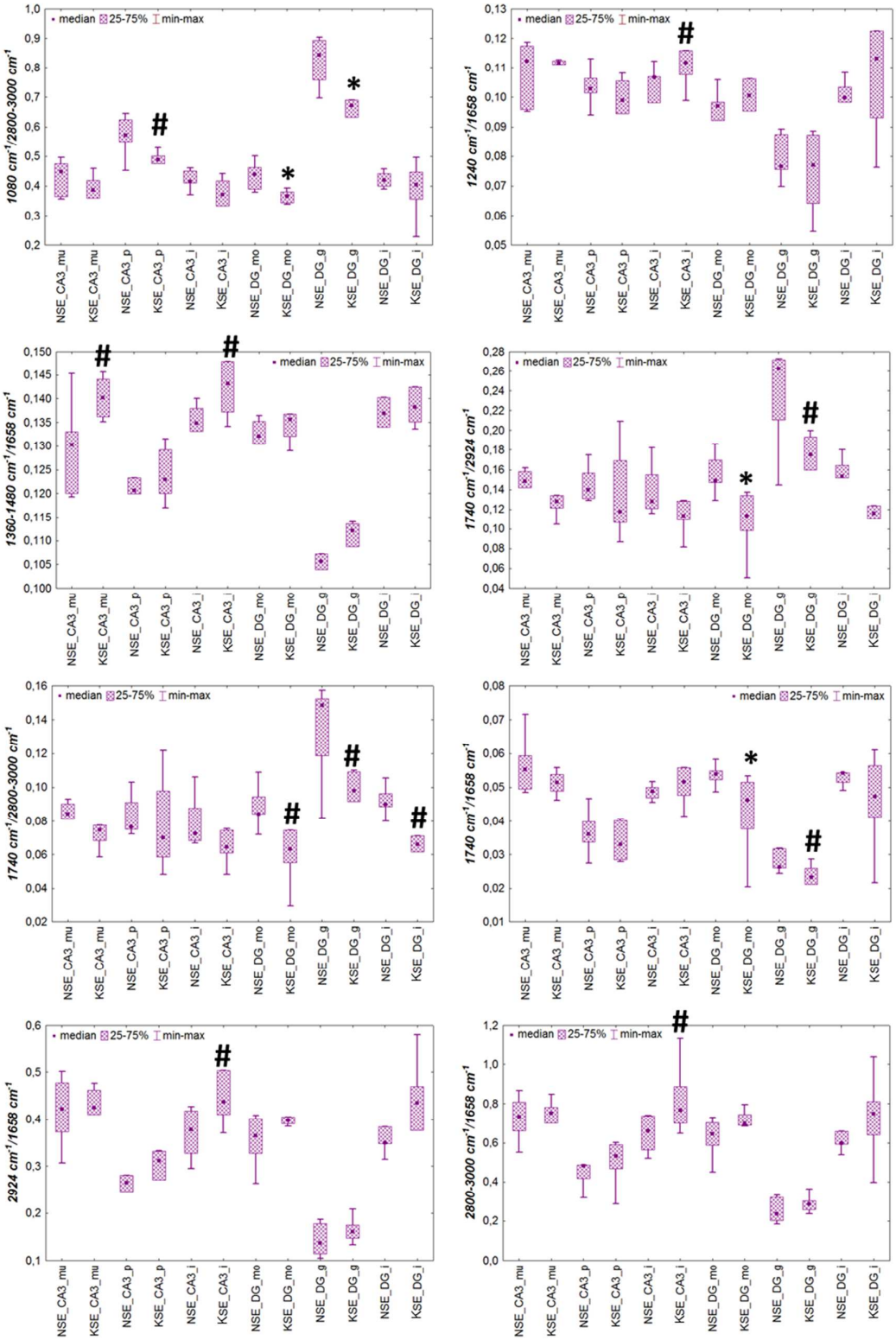

Figure 9b. Median, minimal and maximal values (after the removal of outliers) of biochemical parameters presenting differences between KSE and NSE groups. The cellular layers for which statistically significant changes were observed at the confidence level of 95% were marked with (*) whilst those significant at the confidence level of 90-95% with (#).

Ketogenic diet-induced changes in hippocampal creatine accumulation

Our previous studies on the pilocarpine model of epilepsy showed increased accumulation of creatine deposits in animals experiencing seizures comparing to controls.[18,20] Therefore, we decided to verify how the ketogenic diet modifies the frequency of creatine inclusions within examined hippocampal areas. The median, minimal and maximal numbers of creatine deposits found in CA3 and DG hippocampal areas from all examined animal groups are presented in the Figure 10. Statistically significant differences (verified using U test) between K and N groups were marked with (#), between NSE and N groups with (*) whilst between KSE and K groups with (**).

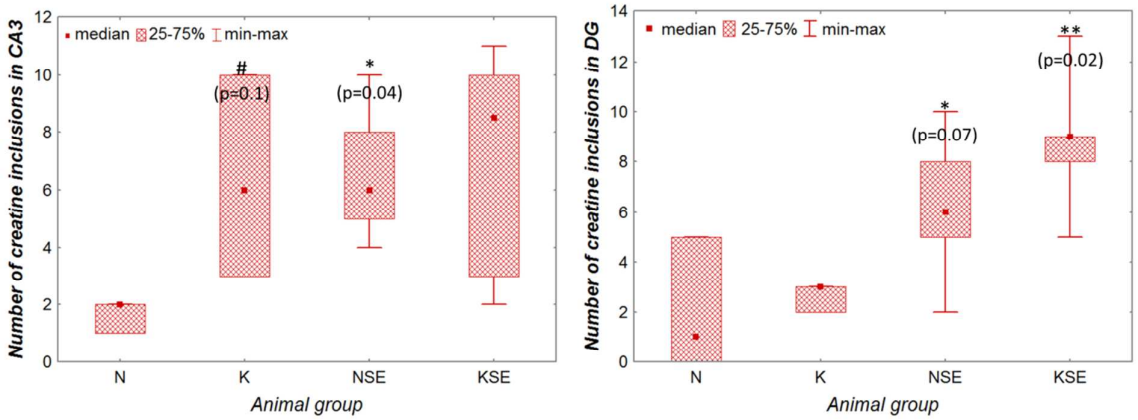

Figure 10. Median, minimal and maximal values (after the removal of outliers) of number of creatine deposits in CA3 and DG hippocampal areas. The statistically significant differences between K and N groups were marked with (#), between NSE and N groups with (*) whilst between KSE and K groups with (**). Additionally *p-values* of U Mann-Whitney tests were shown.

As one can see from the Figure 10, ketogenic diet fed normal animals (K) showed higher frequency of creatine deposits in the CA3 hippocampal area comparing to rats fed with standard diet (N). Such relation was not observed for DG. As a results of seizures evoked in rats on standard diet, the number of inclusions increase in both analyzed regions, and this is in agreement with our previous studies.[18,20] Animals representing KSE and NSE groups did not show any significant differences with respect to creatine accumulation.

Discussion

In the present paper, SRFTIR microspectroscopy was used to verify the influence of ketogenic diet on the biochemical composition of the normal and epileptic hippocampal formation. The comparison of animals on high fat and standard diet showed a few biochemical anomalies that were localized in DG hippocampal area. Higher ratio of absorbance at 1634 and 1658 cm^{-1} was found in internal layer of DG for ketogenic diet fed animals comparing to N group. The mentioned parameter was successfully used in our previous papers as well as in the other studies to detect changes in protein conformation.[14,41,39,40,42] Its elevated level in K group may suggest that ketogenic diet induces structural changes of proteins from α-helix to β-sheet secondary structure.

Moreover, normal animals on ketogenic diet presented elevated intensity of the 1740 cm^{-1} band originating from the stretching vibrations of carbonyl bonds compared to the N group. This anomalie was found for molecular layer of DG and such result is probably an effect of increased accumulation of ketone bodies within the nervous tissue. During ketogenic diet

application free fatty acids present in the blood are transferred into liver. In the mitochondria of liver cells they are degraded in the process of β oxidation what leads to the production of ketone bodies.[51,52,53] All the three types of generated ketone bodies (acetoacetate, aceton and β-hydroxybutyrate) can more easily than glucose cross the blood–brain barrier and therefore may be observed in the hippocampal formations of ketogenic diet fed animals.[52] This could, therefore, be a direct effect of ketogenic diet itself.

The results obtained in the present study confirmed that seizures introduced a number of biochemical changes in the hippocampal formations of rats fed with standard diet.[14,18,20] The anomalies included conformational changes of proteins (increased ratio of absorbances at 1634 and 1658 cm^{-1}), modifications of unsaturation level (3012 cm^{-1}/2924 cm^{-1} and 3012 cm^{-1}/2800-3000 cm^{-1}) of lipids as well as changes in accumulation of biomolecules which were detected as decreased intensity of bands occurring at 1740, 1240 and 1080 cm^{-1}. In contrary to the results of Freitas *et al.*,[54] we did not observe seizure induced changes in hippocampal lipid accumulation. However, increased ratio of intensities of 2924 and 2955 cm^{-1} bands which was observed for NSE animals (in internal layer of CA3) may suggest the occurrence of some structural changes of lipids. They may involve the increase of the fatty acid chains length or decrease of the degree of their branching.[48,49] Unfortunately, an unambiguous interpretation of this parameter is very difficult because it also depends on protein/lipid balance and varies strongly between the nucleus, the cytoplasm and the endoplasmic reticulum/Golgi apparatus.[55,56]

Anomalies in ratios of intensities 3012 cm^{-1}/2924 cm^{-1} and 3012 cm^{-1}/2800-3000 cm^{-1} indicate, moreover, the decrease in the relative content of unsaturated lipids. Seizure evoked changes in the structure and saturation of lipids may suggest that oxidative stress is one of the processes leading to the neurodegenerative changes of hippocampal formation in the pilocarpine model of TLE. Particular vulnerability of the brain to oxidative stress results from the high concentrations of polyunsaturated fatty acids susceptible to peroxidation, large demand for oxygen for energy production and lower antioxidant defense compared to other organs.[57,58,59] Because of high content of polyunsaturated fatty acids, phospholipids constituting a major component of all cell membranes are the main target for oxidative damage induced by hydroxyl, alkoxyl and peroxyl radicals.[60] Moreover, the products of lipid peroxidation: lipid alkoxyl and lipid peroxyl radicals lead to spread of free radical reactions and the same cause further damages to membrane lipid bilayers and mitochondria resulting in severe cellular dysfunction.[61,62,63] An increased level of lipid peroxidation as well as anomalies in the other markers of oxidative stress have been previously described in the pilocarpine model of temporal lobe epilepsy.[64,65,66,67]

To verify the influence of ketogenic diet diet on seizure experiencing brain, KSE and NSE experimental groups were compared. In epileptic animals which were previously fed with ketogenic diet lower ratio of absorbance at 1634 and 1658 cm^{-1} in multiform and internal layers of CA3 was found compared to rats on standard laboratory diet. It suggests that the treatment with high fat diet reduces seizure induced changes in protein conformation.

For some of the examined cellular layers, higher intensity of 2924 cm^{-1} band and increased absorption in the region of lipid massif and the range of wavenumber of 1360-1480 cm^{-1} were detected in KSE comparing to NSE group. The first two parameters point at the elevated accumulation of lipids in seizure experiencing animals on ketogenic diet, whilst the last one may suggest increased cholesterol level. We did not detect differences in unsaturation level between KSE and NSE rats, whilst in DG granular layer, animals on

ketogenic diet treated with pilocarpine presented increased ratio of intensities of 2924 and 2955 cm^{-1} bands.

Similarly as in our previous studies[18,20] creatine deposits were found in hippocampal formations taken from seizure experiencing animals. According to Hackett *et al.*, the formation of such inclusions is a results of creatine crystallization during dehydration of cryomicrotome cut thin tissue sections and this process can be avoided when rapid freezing of brain tissue via decapitation into liquid nitrogen is used instead of perfusion with physiological saline solution.[68,69] From the other side many studies done on animal models or human tissues showed that the frequency of creatine deposits significantly increases in different pathological states of central nervous tissue including Alzheimer's disease, epilepsy and cerebral malaria.[70,71,68,18,20] Therefore, although the formation of crystalline creatine microdeposits may be an *ex vivo* postprocessing artefact, the presence of inclusions identifies tissue regions in which altered metabolism was present *in vivo*.[68] The analysis of the differences in creatine accumulation among the examined animal groups showed that ketogenic diet, similarly as seizures, increased the frequency of creatine deposits in CA3 hippocampal area of normal rats. High fat diet did not influence the number of creatine deposits in seizure experiencing animals.

Conclusions

The results presented in this paper confirmed that highly resolved biochemical analysis of hippocampal formation may be very helpful in the study on the mechanisms underlying a possible neuroprotective action of ketogenic diet in the epileptic brain. The comparison of infrared data obtained for K and N rats showed an increased intensity of 1740 cm^{-1} band what was probably the result of elevated accumulation of ketone bodies within the hippocampal formation tissue of ketogenic diet fed rats. Moreover, increased ratio of absorbance at 1635 and 1658 cm^{-1} in DG and an elevated frequency of creatine deposits in CA3 hippocampal area were found for high fat diet fed animals.

Seizure induced biochemical anomalies recorded for standard diet fed rats confirmed the results presented in our previous papers. The comparison of seizure experiencing rats from KSE and NSE groups showed increased accumulation of lipids and probably cholesterol after ketogenic diet. Moreover, high fat diet reduced seizure induced conformational changes of proteins. The relative content of unsaturated lipids as well as frequency of creatine deposits did not differ between seizure experiencing rats on high fat or standard diet.

Acknowledgements

This work was supported by the Polish Ministry of Science and Higher Education, the Polish National Science Centre grant 2921/B/T02/2011/40 and the Foundation for Polish Science – PARENT-BRIDGE Programme co-financed by the European Union within European Regional Development Fund (POMOST/2013-8/3) and the statutory research of the Institute of Zoology (Jagiellonian University) K/ZDS/004196.

The research leading to these results has received funding from the European Community's Seventh Framework Programme (FP7/2007-2013) CALIPSO under grant agreement number 312284. We also acknowledge SOLEIL for provision of synchrotron radiation facilities (granted proposal IDs: 20110716 and 20120868). We thank also MSc Joanna Osoba for animal care and food delivery.

References

[1]. Sander JW (2003) The epidemiology of epilepsy revisited. Curr Opin Neurol 16:165-170.
[2]. Dichter MA (1994) Emerging insights into mechanisms of epilepsy: implications for new antiepileptic drug development. Epilepsia 35:51-57.
[3]. Banerjee PN, Filippi D, Allen Hauser W (2009) The descriptive epidemiology of epilepsy-a review. Epilepsy Res 85:31-45.
[4]. Dichter MA (2009) Emerging concepts in the pathogenesis of epilepsy and epileptogenesis. Arch Neurol 66:443-447.
[5]. Dichter MA (2009) Posttraumatic epilepsy: the challenge of translating discoveries in the laboratory to pathways to a cure. Epilepsia 50:41-45.
[6]. Kwan P, Schachter SC, Brodie MJ (2011) Drug-resistant epilepsy. N Engl J Med 365:919-926.
[7]. Freeman JM, Vining EP, Kossoff EH, Pyzik PL, Ye X, Goodman SN (2009) A blinded, crossover study of the efficacy of the ketogenic diet. Epilepsia 50:322-325.
[8]. Nabbout R, Mazzuca M, Hubert P, Peudennier S, Allaire C, Flurin V, Aberastury M, Silva W, Dulac O (2010) Epilepsia 51:2033-2037.
[9]. Neal EG, Chaffe H, Schwartz RH, Lawson MS, Edwards N, Fitzsimmons G, Whitney A, Cross JH (2008) Lancet Neurol 7:500-506.
[10]. Henderson CB, Filloux FM, Alder SC, Lyon JL, Caplin DA (2006) J Child Neurol 21:193-198.
[11]. Huffman J, Kossoff EH (2006) Curr Neurol Neurosci Rep 6:332-340.
[12]. Puchowicz MA, Zechel JL, Valerio J, Emancipator DS, Xu K, Pundik S, LaManna JC, Lust WD (2008) J Cereb Blood Flow Metab 28:1907-1916.
[13]. Chwiej J, Winiarski W, Ciarach M, Janeczko K, Lankosz M, Janeczko K, Rickers-Appel K, Setkowicz Z (2008) The role of trace elements in the pathogenesis and progress of pilocarpine-induced epileptic seizures. J Biol Inorg Chem 13:1267-1274.
[14]. Chwiej J, Dulinska J, Janeczko K, Dumas P, Eichert D, Dudala J, Setkowicz Z (2010) Synchrotron FTIR micro-spectroscopy study of the rat hippocampal formation after pilocarpine-evoked seizures, Journal of Chemical Neuroanatomy 40:140-147.
[15]. Chwiej J, Janeczko K, Marciszko M, Czyzycki M, Rickers K, Setkowicz Z (2010) Neuroprotective action of FK-506 (tacrolimus) after seizures induced with pilocarpine: quantitative and topographic elemental analysis of brain tissue. J Biol Inorg Chem 15:283-289.
[16]. Chwiej J, Dulinska J, Janeczko K, Appel K, Setkowicz Z (2012) Variations in elemental compositions of rat hippocampal formation between acute and latent phases of pilocarpine induced epilepsy – an X-ray fluorescence microscopy study. J Biol Inorg Chem 17:731-739.
[17]. Chwiej J, Kutorasinska J, Janeczko K, Gzielo-Jurek K, Uram L, Appel K, Simon R, Setkowicz Z (2012) Progress of elemental anomalies of hippocampal formation in the pilocarpine model of temporal lobe epilepsy – X-ray fluorescence microscopy study. Anal Bioanal Chem 404:3071-3080.
[18]. Dulinska J, Setkowicz Z, Janeczko K, Sandt C, Dumas P, Uram L, Gzielo-Jurek K, Chwiej J (2012) Synchrotron radiation Fourier-transform infrared and Raman microspectroscopy study showing an increased frequency of creatine inclusions in the rat hippocampal formation following pilocarpine-induced seizures. Anal Bioanal Chem 402:2267-2274.
[19]. Dudała J, Janeczko K, Setkowicz Z, Eichert D, Chwiej J (2012) The use of SR-FTIR microspectroscopy for a preliminary biochemical study of the rat hippocampal formation

tissue in case of pilocarpine induced epilepsy and neutroprotection with FK-506. Nukleonika 57:615-619.

[20]. Kutorasinska J, Setkowicz Z, Janeczko K, Sandt C, Dumas P, Chwiej J (2013) Differences in the hippocampal frequency of creatine inclusions between the acute and latent phases of pilocarpine model defined using synchrotron radiation-based FTIR microspectroscopy. 405:7337-7345.

[21]. Dumas P, Sockalingum GD, Sulé-Suso J (2007) Adding synchrotron radiation to infrared microspectroscopy: what's new in biomedical applications? Trends Biotechnol 25:40-44.

[22]. Miller LM, Dumas P (2010) From structure to cellular mechanism with infrared microspectroscopy. Curr Opin Struct Biol 20:1-8.

[23]. Ali K, Lu Y, Das U, Sharma RK, Wiebe S, Meguro K, Sadanand V, Fourney DR, Vitali A, Kelly M, May T, Gomez J, Pellerin E (2010) Biomolecular diagnosis of human glioblastoma multiforme using synchrotron mid-infrared spectromicroscopy. Int J Mol Med 26:11-16.

[24]. El Bedewi A, El Anany G, El Mofty M, Kretlow A, Park S, Miller LM (2010) The use of synchrotron infrared microspectroscopy in the assessment of cutaneous T-cell lymphoma vs. pityriasis lichenoides chronic. Photodermatol Photoimmunol Photomed 26:93-97.

[25]. Le Naour F, Bralet MP, Debois D, Sandt C, Guettier C, Dumas P, Brunelle A, Laprévote O (2009) Chemical imaging on liver steatosis using synchrotron infrared and ToF-SIMS microspectroscopies. PLoS One 4:e7408.

[26]. Leskovjan AC, Lanzirotti A, Miller LM (2009) Amyloid plaques in PSAPP mice bind less metal than plaques in human Alzheimer's disease. Neuroimage 47:1215-1220.

[27]. Setkowicz Z, Kłak K, Janeczko K (2003) Long-term changes in postnatal susceptibility to pilocarpine-induced seizures in rats exposed to gamma radiation at different stages of prenatal development. Epilepsia 44:1267–1273.

[28]. Racine RJ (1972) Modification of seizure activity by electrical stimulation: II. Motor seizure. Electroencephalogr Clin Neurophysiol 32:281-294.

[29]. Paxinos G, Watson C (1989) The rat brain in stereotaxic coordinates. Academic Press, Australia.

[30]. Martin FL, Kelly JG, Llabjani V, Martin-Hirsch PL, Patel II, Trevisan J, Fullwood NJ, Walsh MJ (2010) Application of infrared spectroscopy to distinguish cell types or populations based on the derivation and computation analyses of a biochemical-cell fingerprint. Nature Protocols 5:1748-1760.

[31]. Filik J, Frogley MD, Pijanka JK, Wehbe K, Cinque G (2012) Electric field standing wave artefacts in FTIR micro-spectroscopy of biological materials. Analyst 137:853-861.

[32]. Wehbe K, Filik J, Frogley MD, Cinque G (2013) The effect of optical substrates on micro-FTIR analysis of single mammalian cells. Anal Bioanal Chem 405:1311-1324.

[33]. Bassan P, Lee J, Sachdeva A, Pissardini J, Dorling KM, Fletcher JS, Henderson A, Gardner P (2013) The inherent problem of transflection-mode infrared spectroscopic microscopy and the ramifications for biomedical single point and imaging applications. Analyst 138:144-157.

[34]. Lasch P, Haensch W, Naumann D, Diem M (2004) Imaging of colorectal adenocarcinoma using FT-IR microspectroscopy and cluster analysis. Biochim Biophys Ac 1688:176-186.

[35]. Bassan P, Kohler A, Martens H, Lee J, Byrne H J, Dumas P, Gazi E, Brown M, Clarke N, Gardner P (2010) Resonant Mie Scattering (RmieS) correction of infrared spectra from highly scattering biological sample. Analyst 135:268-277.

[36]. Stuart B (2004) Infrared spectroscopy: fundamentals and applications. John Wiley & Sons Ltd, England.

[37]. Dreissig I, Machill S, Salzer R, Krafft C (2009) Quantification of brain lipids by FTIR spectroscopy and partial least squares regression. Spectrochim Acta A Mol Biomol Spectrosc 71:2069-2075.
[38]. Kneipp J, Lasch P, Baldauf, E., Beekes M, Naumann D (2000) Detection of pathological molecular alterations in scrapie-infected hamster brain by Fourier transform infrared (FT-IR) spectroscopy. Biochim Biophys Ac 1501:189-199.
[39]. Miller LM, Wang Q, Telivala T, Smith R, Lanzirotti A, Miklossy J (2006) Synchrotron-based infrared and X-ray imaging shows focalized accumulation of Cu and Zn co-localized with β-Amyloid deposits in Alzheimer's disease. J Struct Biol 155:30-37.
[40]. Kretlow A, Wang Q, Kneipp J, Lasch P, Beekes M, Miller L, Naumann D (2006) FTIR-microspectroscopy of prion-infected nervous tissue. Biochim Biophys Ac 1758:948-959.
[41]. Szczerbowska-Boruchowska M, Dumas P, Kastyak MZ, Chwiej J, Lankosz M, Adamek D, Krygowska-Wajs A (2007) Biomolecular investigation of human substantia nigra in Parkinson's disease by synchrotron radiation Fourier transform infrared microspectroscopy. Arch Biochem Biophys 459:241-248.
[42]. Kneipp J, Miller L, Joncic M, Kittel M, Lasch P, Beekes M, Naumann D (2003) In situ identification of protein structural changes in prion-infected tissue. Biochim Biophys Ac 1639:152-158.
[43]. Diem M, Boydston-White S, Chiriboga L (1999) Infrared spectroscopy of cells and tissues: shining light onto a novel subject. Appl Spectrosc 53:148-161.
[44]. Liquier J, Taillandier R (1996) Infrared spectroscopy of nucleic acids. In: Mantsch HH, Chapman D (eds) Infrared Spectroscopy of Biological Molecules. Wiley-Liss, New York, pp. 131-158.
[45]. NIST Standard Reference Database Number 69: http://webbook.nist.gov/chemistry/.
[46]. Petibois C, Deleris G (2005) Evidence that erythrocytes are highly susceptible to exercise oxidative stress: a FT-IR spectrometry study at the molecular level. Cell Biol Int 29:709-716.
[47]. Petibois C, Deleris G (2006) Chemical mapping of tumor progression by FT-IR imaging: towards molecular histopathology. Trends in Biotechnology 24:455-462.
[48]. Kretlow A (2007) Imaging molecular and trace element changes in scrapie-infected nervous tissue with a time course study. Doctoral dissertation, Free University of Berlin, Germany.
[49]. Dogan A, Lasch P, Neuschl C, Millrose MK, Alberts R, Schughart K, Naumann D, Brockmann GA (2013) ATR-FTIR spectroscopy reveals genomic loci regulating the tissue response in high fat diet fed BXD recombinant inbred mouse strains. BMC Genomics 14:386.
[50]. Gallant M, Rak M, Szeghalmi A, Del Bigio MR, Westaway D, Yang J, Julian R, Gough KM (2006) Focally elevated creatine detected in amyloid precursor protein (APP) transgenic mice and Alzheimer disease brain tissue. Journal of Biological Chemistry 281:5-8.
[51]. Gasior M, Rogawski MA, Hartman AL (2006) Neuroprotective and disease-modifying effects of the ketogenic diet. Behavioural Pharmacology 17:431-439.
[52]. Politi K, Shemer-Meiri L, Shuper A, Aharoni S (2011) The ketogenic diet 2011: how it works. Epilepsy Research and Treatment 2011:963637.
[53]. Bough KJ and Rho JM (2007) Anticonvulsantmechanisms of the ketogenic diet. Epilepsia 48:43-58.
[54]. Freitas RM, Nascimento KG, Ferreira PMP, Jordan J (2010) Neurochemical changes on oxidative stress in rat hippocampus during acute phase of pilocarpine-induced seizures. Pharmacology Biochemistry and Behaviour 94:341-345.

[55]. Gazi E, Dwyer J, Lockyer NP, Miyan J, Gardner P, Hart C, Brown M, Clarke NW (2005) Fixation protocols for subcellular imaging by synchrotron-based Fourier transform infrared microspectroscopy. Biopolymers 77:18-30.
[56]. Sandt C, Frederick J, Dumas P (2013) Profiling pluripotent stem cells and organelles using synchrotron radiation infrared microspectroscopy. Journal of Biophotonics 6:60-72.
[57]. Adibhatla RM, Hatcher JF (2007) Role of Lipids in Brain Injury and Diseases. Future Lipidology 2:403-422.
[58]. Frantseva MV, Velazquez JL, Hwang PA, Carlen PL (2000) Free radical production correlates with cell death in a vitro model of epilepsy. European Journal of Neuroscience 12:1431-1439.
[59]. Bellissimo MI, Amado D, Abdalla DS, Ferreira EC, Cavalheiro EA, Naffah-Mazzacoratti MG (2001) Superoxide dismutase, glutathione peroxidase activities and the hydroperoxide concentration are modified in the hippocampus of epileptic rats. Epilepsy Research 46:121-128.
[60]. Gutteridge JMC (1988) Lipid peroxidation: some problems and concepts. In: Halliwell B (ed.), Oxygen Radicals and Tissue Injury. FASEB, Bethesda, pp. 9-19.
[61]. Nigam S, Schewe T (2000) Phospholipase A(2)s and lipid peroxidation. Biochimica Biophysica Acta 1488:167-181.
[62]. Green DR, Reed JC (2000) Mitochondria and apoptosis. Science 281:1309-1312.
[63]. Catalá A (2006) An overview of lipid peroxidation with emphasis in outer segments of photoreceptors and the chemiluminescence assay. International Journal of Biochemistry and Cell Biology 38:1482-1495.
[64]. Freitas RM, Souza FCF, Vasconcelos SMM, Viana GSB, Fonteles MMF (2005) Oxidative stress in the hippocampus after status epilepticus in rats. FEBS Journal 272:1307-1312.
[65]. Freitas RM (2009) Investigation of oxidative stress involvement in hippocampus in epilepsy model induced by pilocarpine. Neuroscience Letters 462:225-229.
[66]. Tejada S, Roca C, Sureda A, Rial RV, Gamundí A, Esteban S (2006) Antioxidant response analysis in the brain after pilocarpine treatments. Brain Research Bulletin 69:587-592.
[67]. Tejada S, Sureda A, Roca C, Gamundi A, Esteban S (2007) Antioxidant response and oxidative damage in brain cortex after high dose of pilocarpine. Brain Research Bulletin 71:372-375.
[68]. Hackett MJ, Lee J, El-Assaad F, McQuillan JA, Carter EA, Grau GE, Hunt NH, Lay PA (2012) FTIR imaging of brain tissue reveals crystalline creatine deposits are an ex vivo marker of localized ischemia during murine cerebral malaria: general implications for disease neurochemistry. ACS Chemical Neuroscience 3:1017-1024.
[69]. Hackett MJ, Britz CJ, Paterson PG, Nichol H, Pickering IJ, George GN (2014) In Situ Biospectroscopic Investigation of Rapid Ischemic and Postmortem Induced Biochemical Alterations in the Rat Brain. ACS Chemical Neuroscience [Epub ahead of print].
[70]. Gallant M, Rak M, Szeghalmi A, Del Bigio MR, Westaway D, Yang J, Julian R, Gough KM (2006) J BiolChem 281:5-8.
[71]. Burklen TS, Schlattner U, Homayouni R, Gough K, Rak M, Szeghalmi A, Wallimann T (2006) J Biomed Biotech 2006:1-11